arXiv:0704.3328v1 [astro-ph] 25 Apr 2007

A SUBARU/SUPRIME-CAM SURVEY OF M31'S SPHEROID ALONG THE SOUTH-EAST MINOR AXIS[1]

Mikito Tanaka[2,3], Masashi Chiba[4], Yutaka Komiyama[2], Masanori Iye[2], and Puragra Guhathakurta[5]

Draft version February 1, 2008

ABSTRACT

We have used Suprime-Cam on the Subaru Telescope to conduct a V- and I-band imaging survey of fields sampling the spheroid of the Andromeda galaxy along its south-east minor axis. Our photometric data are deep enough to resolve stars down to the red clump. Based on a large and reliable sample of red giant stars available from this deep wide-field imager, we have derived metallicity distributions vs. radius and a surface brightness profile over projected distances of $R = 23$–66 kpc from the galaxy's center. The metallicity distributions across this region shows a clear high mean metallicity and a broad distribution ([Fe/H]$\sim -0.6 \pm 0.5$), and indicates no metallicity gradient within our observed range. The surface brightness profile at $R > 40$ kpc is found to be flatter than previously thought. It is conceivable that this part of the halo samples as yet unidentified, metal-rich substructure.

Subject headings: galaxies: individual (M31) — galaxies: halos — galaxies: structure

1. INTRODUCTION

Our understanding of how disk galaxies like our own or the Andromeda galaxy (M31) formed plays a key role in near-field cosmology (Freeman & Bland-Hawthorn 2002), because such nearby galaxies offer us detailed views of galactic structures through their resolved stars. In particular, the components of the extended low surface brightness stellar halo, old field stars and globular clusters, provide invaluable information on early chemo-dynamical evolution of disk galaxies over the past $\gtrsim 10$ Gyr (i.e., well before thin disk components appeared). The spatial distribution of galactic halos suggests that proto-galaxies were much larger than the sizes of currently bright galactic disks, possibly a result of hierarchical assembly of subgalactic systems orbiting at larger radii (Searle & Zinn 1978). The importance of accretion and merging of small systems in the galaxy formation process is also evident in the spatial and kinematic substructures in the Galaxy's stellar halo (e.g., Yanny et al. 2003; Helmi et al. 1999).

The volume density profile of the Milky Way halo is characterized by an $r^{-3.5}$ power-law of Galactocentric radius, based on direct counts of halo tracers or their orbital motions (e.g., Harris 1976). By contrast, Andromeda's spheroid appears to have a complex structure. In their imaging study Pritchet & van den Bergh (1994) found that the surface brightness (SB) profile along the minor axis is characterized by a de Vaucouleurs $R^{1/4}$ law over projected distances R of $1''$ to $1°.5$ (few pc to 20 kpc) from the M31 center. Later, Guhathakurta et al. (2005) reported, based on spectroscopic selection of red giant branch (RGB) candidates in several halo fields, that

the SB beyond $R \simeq 20$ kpc shows a flatter profile with $R^{-2.3}$, and that the halo may extend to $R \gtrsim 150$ kpc. Irwin et al. (2005) also found, from their photometry of RGB stars over $R = 20$–55 kpc along the minor axis, a comparably flat SB profile that is fit by an $R^{-2.3}$ power law or an exponential law with a scalelength of 14 kpc. It remains to be seen whether this flat portion of the halo profile is affected by substructure, and if it is dominated by either metal-rich or metal-poor populations. The latter issue is especially important since spectroscopic studies suggest that M31's inner spheroid/halo has a radial gradient in mean metallicity, whereby metal-poor stars dominate at $R \gtrsim 50$ kpc (e.g., Kalirai et al. 2006). Detailed studies based on large numbers of stars (say from wide-field imagers) are required to investigate the fundamental nature of M31's halo along its minor axis.

In this Letter, we report on our Subaru/Suprime-Cam wide-field photometric observations of M31's halo aimed at obtaining statistically significant SB and metallicity distribution (MD) profiles along the south-east (SE) minor axis of the galaxy. Our imaging survey is optimized to extract halo profiles in a region that is well outside the bright disk component and beyond the inner spheroid with the $R^{1/4}$ brightness law.

2. OBSERVATIONS AND DATA REDUCTIONS

Using the Suprime-Cam (Miyazaki et al. 2002) imager on the Subaru Telescope (Iye et al. 2004), which consists of ten 2000×4000 CCDs with a resolution of $0''.202$ per pixel and covers a total field-of-view $34' \times 27'$, we have carried out a wide-field imaging survey of M31's spheroid. Our targeted fields are located between 23 and 66 kpc from the M31 center (Fig. 1).

During four nights in August 2004, we obtained images of seven spheroid fields (hereafter referred to as Fields 1–7) and a control field in Johnson V and Cousins I bands with typical seeing FWHM of $0''.9 - 1''.3$. These observations were obtained in non-photometric conditions. We carried out additional imaging of the same fields on a photometric night in August 2005 in order to calibrate the data. The data were reduced with the software package SDFRED, a useful pipeline developed to optimally deal with Suprime-Cam images (Yagi et al. 2002;
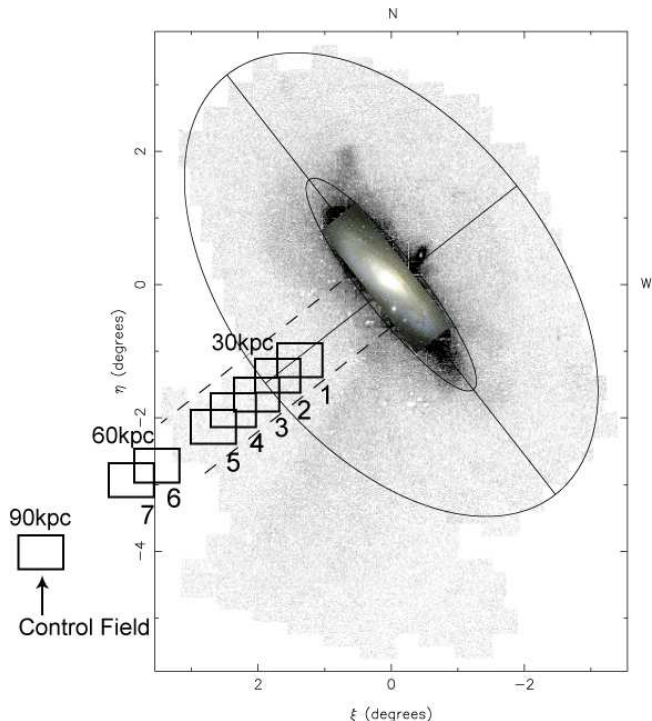
FIG. 1.— Locations of our Subaru/Suprime-Cam fields (rectangular areas), overlaid on the surface density map of M31's red RGB stars from the INT/WFC survey of Ferguson et al. (2002) and adapted from Figure 1 of Irwin et al. (2005). Adjacent Suprime-Cam fields overlap by about 25 % to ensure photometric calibration. In addition, the fields used by Irwin et al. (2005) for their surface brightness profile are delineated by the dashed lines.

FIG. 2.— Histograms of the metallicity distributions, in the Carretta & Gratton (1997) scale, for the SE minor axis fields of M31's spheroid. In the upper left corner of each panel, we show the name of the field, the number of stars used to derive the MD, the average metallicity ($[Fe/H]_{ave}$) together with the associated standard deviation, and the median metallicity together with the associated semiinterquartile interval.

Ouchi et al. 2004). Photometry of our co-added images was calibrated through Landolt (1992) standards, correcting for an airmass term and a color term in each field.

We then conducted PSF-fitting photometry using the IRAF version of the DAOPHOT-II software (Stetson 1987). We adopted a $3\,\sigma$ detection threshold for the initial object detection/photometry pass and iterated the PSF-fitting photometry twice with $5\,\sigma$ and $7\,\sigma$ detection thresholds, respectively, in order to account for blended stars. A stellar PSF template was derived from about 100 bright, isolated stars per image. Finally, we merged two independent V- and I-band catalogs into a combined catalog using a 1-pixel matching radius.

It is worth noting that the morphological segregation method cannot distinguish between M31 halo stars and and other point sources such as Galactic foreground dwarf stars, and compact extragalactic objects. To statistically remove these contaminations from the targeted fields, we adopted a control field located at a Galactic latitude comparable to that of our targeted fields, on the assumption that it has the same abundance of foreground and background objects as that in the M31 spheroid fields.

Reddening corrections are applied in each field based on the extinction maps of Schlegel et al. (1998), and the Dean et al. (1978) reddening law $E(V-I) = 1.34E(B-V)$ and $A_I = 1.31E(V-I)$. We adopt the M31 Cepheid distance modulus of $(m-M)_0 = 24.43 \pm 0.06$ (~ 770 kpc) from Madore & Freedman (1995). We also note that our analysis of the SB and MD profiles below is unaffected by photometric incompleteness: we target RGB
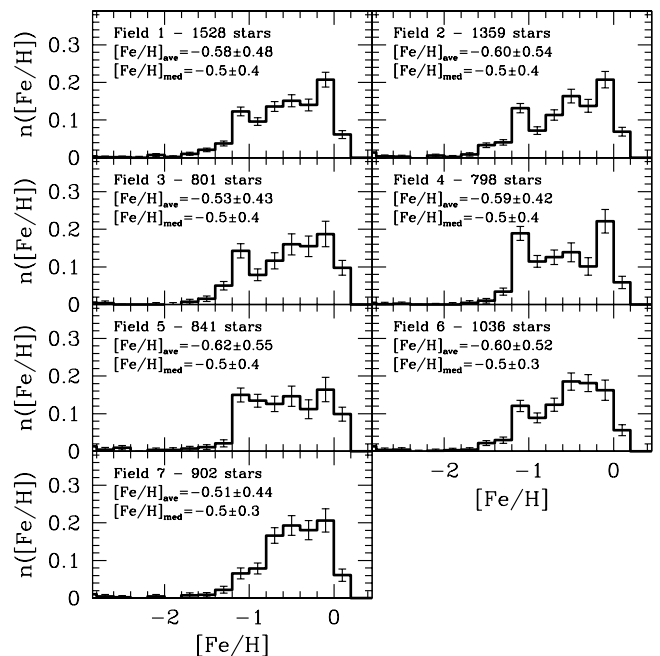
stars brighter than $I \sim 22.5$ (mag), while our data are more than 90% complete down to $I \sim 23$ (mag). As an example, even if we count stars down to the 50% completeness for the V band, the hitherto missing faintest and reddest stars are included in the analysis but the SB and MD profiles are changed by less than a few percent.

3. RESULTS

3.1. *Metallicity Distributions*

Taking advantage of the large stellar samples available with the wide field of view of Suprime-Cam, we derive MDs of RGB stars in M31's spheroid, by comparing them to RGB fiducials defined by Galactic globular clusters in the same manner as Bellazzini et al. (2003). For a reliable secure determination of MDs using these templates, we select RGB stars with $-3.8 < M_I < -2.0$ and $0.9 < (V-I)_0 < 4.0$. These selection criteria allow us to remove a number of contaminants, such as M31 asymptotic giant branch (AGB) stars, AGB bump stars, and young stars, along with foreground and background objects. We perform an interpolation procedure to obtain metallicities of objects in the spheroid and control fields, and subtract the derived MD of the control field from that of the spheroid field in order to statistically remove the effects of the foreground and background contaminants. For more detailed description, see Tanaka et al. (2007).

Figure 2 shows the MDs in Fields 1 to 7 of M31's spheroid. The vertical error bars denote a nominal uncertainty in each metallicity bin, yielding from the Poisson errors equal to $\pm\sqrt{N(\text{spheroid} + \text{control})}$. It is worth noting that because of a large number of the RGB stars available from our Suprime-Cam data, the MDs obtained here have significantly small errors and thus are expected
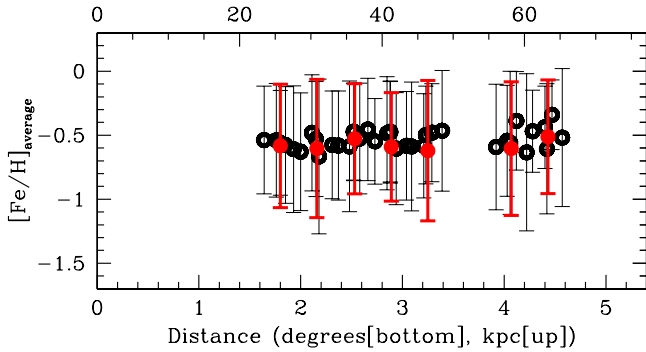
FIG. 3.— The average metallicity plotted as a function of distance from the M31 center. Filled red circles present the average values of metallicity in the seven targeted fields, while open circles denote those in each subfield inside a Suprime-Cam field (see text).

to be most likely compared with the results of the previous studies, which examined more inner parts of the spheroid than ours (Durrell et al. 2001; Bellazzini et al. 2003; Durrell et al. 2004).

It follows that the MDs have a broad distribution ranging from [Fe/H] ~ -3 to the near solar metallicity. The average metallicity ([Fe/H]$_{\rm ave}$) with a standard deviation and median metallicity ([Fe/H]$_{\rm med}$) with a quartile deviation are shown in each panel. In addition, our Field 2 includes the field observed by Durrell et al. (2004), and the MD of Field 2 is almost consistent with their MD.

The most striking feature of the MDs shown in Fig. 2 is their overall similarity. For the sake of comparison of them, we show their average metallicities as a function of distance from the M31 center in Figure 3. Seven filled red circles present the average values of metallicity in our targeted fields, while many open circles are those in the subfields, which are obtained by dividing a single Suprime-Cam field into six fields (4000 pixels × 3000 pixels per divided field). These subfields help us to examine the fine spatial variation in a Suprime-Cam field. Conversely, a filled red circle reflects the mean value of metallicities of six subfields. Vertical error bars show standard deviation of the mean. These plot suggests that the stellar content of the spheroid has no metallicity gradient within our observational range. This may be consistent with the idea of chaotic merging of small building blocks first proposed by Searle & Zinn (1978) for understanding the lack of a metallicity gradient in the globular cluster system of the Milky Way halo.

3.2. *Surface Brightness Profiles*

We estimate the SB profiles of M31's spheroid along the SE minor axis using the RGB stars, which are brighter than the AGB bump ($I \sim 23.3$ mag). After extracting the secure RGB stars on which are imposed the same magnitude and color criteria as in preceding section, we divide them into the following two groups using the RGB templates of Galactic globular clusters (Bellazzini et al. 2003): *Metal-Poor group* (MP) defined as $-2.16 <$[Fe/H]< -1.11 and *Metal-Rich group* (MR) defined as $-1.11 <$[Fe/H]< 0.07. The values of -2.16 and 0.07 are both ends of the templates, and the template having a value of -1.11 is chosen because it nearly marks a discontinuity in the MDs obtained here.

In contrast to the inner dense parts of the halo in M31, it is possible to resolve the individual stars in its outer parts, because of their sparse density and of the suffi-
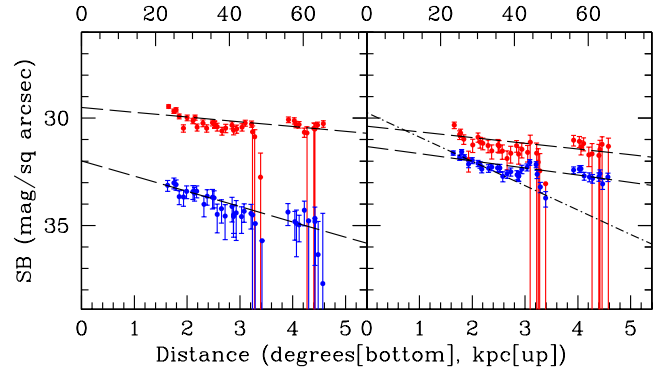

FIG. 4.— The left panel shows the V- and I-band minor-axis profiles for RGB stars as derived from the MP and MR group, while the right panel shows those based on the selection method of RGB stars by Irwin et al. (2005). The V-band and I-band profiles are illustrated with blue and red points, respectively, which are derived from star counts in the magnitude and color selection boxes as described in the text. The error bars reflect a combination of Poissonian and background uncertainties. The dashed lines show an exponential profile with a scalelength of $s = 21.9$ kpc for MP and $s = 70.0$ kpc for MR (left panel), and $s = 46.4$ kpc for blue RGB stars and $s = 58.5$ kpc for red RGB stars (right panel). The dot-dashed line in the right panel shows an exponential profile with $s = 13.7$ kpc by Irwin et al. (2005), for the sake of comparison.

ciently close distance of M31 to us. Thus the SB profiles in spheroid's outer part are available by directly counting individual stars. The sources of noise in this method of estimating the SBs arise from the Poisson statistics from the finite number of stars observed and contamination from Galactic stars along the line of sight to the spheroid. The contribution from unrelated Galactic stars can be estimated by observing other nearby fields: we use our control field at ~ 90 kpc to this end.

The left panel of Figure 4 shows the SB profiles of the MP (blue) and MR (red) group, which are used to derive the V- and I-band profiles, respectively. The dashed lines show an exponential SB profile, $\exp(-R/s)$, with a scale length s of 21.9 kpc for MP and 70.0 kpc for MR. We note that at large distances R, the number of RGB stars is just slightly larger than that of background objects, so we can determine only the upper limit for the most of their errors. It is remarkable that the SB in the MP group decreases more steeply with R than that in the MR group, suggesting that as above stated there may exist a metal-rich substructure at $R = 50 \sim 60$ kpc.

The right panel of Fig. 4 shows the SB profiles based on the different star selection by Irwin et al. (2005): using V-band and Gunn i-band systems, they selected blue RGB stars with $20.5 < i < 22.5$ and $24.85 - 2.85(V - i) < i < 26.85 - 2.85(V - i)$ and red RGB stars with $21 < i < 22$ and $i > 26.85 - 2.85(V - i)$, and derived the V- and I-band profiles from these categorized stars, respectively. We shift I-band magnitude criterion about 0.02 mag toward the fainter side in order to match the Gunn i-band system. We note that our selection criteria for MP and MR are more advantageous than this fixed magnitude and color selection of blue and red RGB stars for investigating the effects of the MDs on the SBs. To compare with the blue RGB star count profile in Irwin et al. (2005), which is fitted to an exponential profile with $s = 13.7$ kpc, we shift it vertically to roughly overlap with our blue RGB surface brightness profile in the radial range $1°\!6 - 3°\!0$. This result shows that stellar density at around 45 kpc and 60 kpc significantly ex-

ceeds a mean halo profile obtained by Irwin et al. (2005). Hence, it is possible that two as-yet-unknown substructures consist of bright metal-rich stars.

We note that the details of the SB profiles obtained here are found to be pretty insensitive even if we adopt much fainter V- and I-band magnitude limits, say down to $V = 25$ mag and $I = 24$ mag. Thus, the current results are real and robust against the effects of any contaminations over the fields; our deep Suprime-Cam data enable us to assess the minor effects of these errors.

4. DISCUSSION AND CONCLUSIONS

As fossil records of galaxy formation, M31's spheroid offers us a global perspective about its spatial structures as well as stellar populations. Based on a wide-field imager of Subaru, we have confirmed the previous results (Guhathakurta et al. 2005; Irwin et al. 2005) that the SB profile in the SE minor axis is much flatter at $R > 23$ kpc than the innermost part of the spheroid described by the $R^{1/4}$ law. Our finding of no metallicity gradient in this outer part over $R = 23 \sim 66$ kpc implies that dissipationless processes, such as accretion and merging of collisionless stellar systems, may have been at work for the formation of this spheroidal part, thereby erasing any metallicity nonuniformity. We note here that our control field at $R = 90$ kpc of the SE minor axis, which shows no substructures (Ibata et al. 2007), may still contain some spheroidal stars, because M31's spheroid may extend up to $R \sim 150$ kpc (Guhathakurta et al. 2005). However, even so, the relative MD and SB profiles obtained here remain unaltered.

Intriguingly, our finding of the possible overdensity regions at around 45 and 60 kpc is in agreement with the recent work by Ibata et al. (2007) (having appeared in astro-ph while preparing for the submission of our paper), who also found the stream-like features at similar locations, referred to as stream D and C, respectively. Our metallicity analysis suggests that their stream D appears to be slightly more metal-poor than stream C. Also, the MDs of stream C (our Field 6 and 7) have a high-metallicity peak similar to those of the Giant Stream (Tanaka et al. 2007). However, it is yet uncertain if stream C is indeed related to the Giant Stream because of the lack of the information on the distance to stream C as well as its internal kinematics. Deeper photometry down to horizontal-branch magnitude and/or multi-object spectroscopy of stars will be important for clarifying the origin of the newly detected substructures.

Our results reported here are not totally inconsistent with the finding by Kalirai et al. (2006) and Chapman et al. (2006), who argue for the presence of metallicity gradient obtained from their kinematical studies of the bright RGB stars using Keck/DEIMOS. Indeed, only our Field 2 overlaps Field a0 of Kalirai et al. (2006), where both fields yield basically similar metallicity, and other fields of Field 2 to 7 along the minor axis do not overlap their survey regions (see their Figures 1 and 12). It is interesting to remark that their Field m6 at $R \simeq 87$ kpc along the minor axis shows rather high metallicity of [Fe/H]~ -0.85, being similar to that of their Field a0 as well as ours. In contrast, other fields deviated from the minor axis (such as their a13, a19, and b15) show low metallicities, which basically give rise to the reported metallicity gradient. Thus, this implies that the MDs along the minor axis fields in concern may be somewhat different from other outer halo fields, i.e., more higher surface density and more metal-rich than previously thought as reported here. A tempting view for these properties of our observed fields is that there exists a metal-rich substructure at R of 50-60 kpc, corresponding to a faint tail of the giant stellar stream (Ferguson et al. 2002) or a part of another stream. More extensive studies by observing large halo areas of Andromeda, e.g., using much wider HyperSuprime camera under construction, will be necessary to arrive at more decisive conclusions and thus obtain the accurate formation picture of this typical disk galaxy.

REFERENCES

Bellazzini, M., et al. 2003, A&A, 405, 867
Carretta, E. & Gratton, R. 1997, A&AS, 121, 95
Chapman, S. C., et al. 2006, ApJ, 653, 255
Dean, J. F., Warren, P. R., & Cousins, A. W. J. 1978, MNRAS, 183, 569
Durrell, P. R., Harris, W. E., & Pritchet, C. J. 2001, AJ, 121, 2557
Durrell, P. R., Harris, W. E., & Pritchet, C. J. 2004, AJ, 128, 260
Ferguson, A. M. N., et al. 2002, AJ, 124, 1452
Freeman, K., & Bland-Hawthorn, J. 2002, ARA&A, 40, 487
Guhathakurta, P., et al. 2005, astro-ph/0502366
Harris, W. E. 1976, AJ, 81, 1095
Helmi, A., et al. 1999, Nature, 402, 53
Ibata, R., et al. 2007, astro-ph/0704.1318
Irwin, M., et al. 2005, ApJ, 628, L105
Iye, M., et al. 2004, PASJ, 54, 833

Kalirai, J. S., et al. 2006, ApJ, 648, 389
Landolt, Arlo U. 1992, AJ, 104, 340
Madore, B. F., & Freedman, W. L. 1995, AJ, 109, 1645
Miyazaki, S., et al. 2002, PASJ, 54, 833
Ouchi et al. 2004, ApJ, 611, 660
Pritchet, C. J., & van den Bergh, S. 1994, AJ, 107, 1730
Schlegel, D. J., Finkbeiner, D. P., & Davis, M. 1998, ApJ, 500, 525
Searle, L., & Zinn, R. 1978, ApJ, 225, 357
Stetson, P. 1987, PASP, 99, 191
Tanaka, M., et al. 2007, preprint (to be submitted to AJ)
Yagi, M., et al. 2002, AJ, 123, 66
Yanny, B., et al. 2003, ApJ, 588, 824